

# Isolation Improvement Using the Field-Circuit Combined Method for In-Band Full-Duplex MIMO Antenna Arrays

Yiran Da, Jianjia Yi, Jianxing Li, and Xiaoming Chen

School of Information and Communications Engineering  
Xi'an Jiaotong University, Xi'an, 710049, China  
dyr916@stu.xjtu.edu.cn, xiaoming.chen@mail.xjtu.edu.cn

**Abstract** – This paper proposes a field-circuit combined decoupling method for co-polarized in-band full-duplex multiple-input multiple-output (MIMO) antenna arrays. The proposed field-circuit combined method is composed of decoupling network and neutralization-based decoupling. An in-band full-duplex antenna with high isolation and low cross-polarization level is designed and extended to a  $1 \times 4$  linear array. The decoupling network and ADS are applied for the array to alleviate the mutual coupling by rebuilding the neutralization wave paths in the circuit and field domains. Thus, low coupling ( $< -25$  dB) among the transmitting/receiving antennas and high isolation ( $> 47$  dB) between the transmitting and receiving antennas are achieved at 2.6 GHz, exhibiting a superior decoupling performance.

**Index Terms** – antenna array, decoupling, field-circuit combined, in-band full-duplex.

## I. INTRODUCTION

With the increasing demand for wireless communication systems, full-duplex communication was developed for higher spectrum efficiency [1, 2]. In-band full-duplex antennas have been studied for base station applications [3, 4], which can transmit and receive signals simultaneously in the same frequency band. When full-duplex antennas are used in MIMO antenna arrays, the antenna elements are closely arranged due to the limited space. Signal interference is generated between the receiving and transmitting antennas, and mutual coupling is generated between the receiving/transmitting antennas, which significantly deteriorate the performances of the wireless communication systems (including receiver performance, error rate, dynamic range, and channel capacity) [5–7]. Notably, 100 dB isolation between the transmitter and receiver is generally required for full-duplex systems, which is usually achieved by combining the antenna, analog and digital domains [8, 9]. Therefore, the isolation at antenna level should be improved as much as possible to reduce the order of the analog radio

frequency filters, thus facilitating the subsequent design of the communication system. Furthermore, mutual coupling (among the transmitting/receiving antennas) below  $-25$  dB is sufficient for MIMO arrays.

Various methods have been studied for suppressing the mutual couplings. The first type is the field domain decoupling method, which is classified into two categories of partition and neutralization. Decoupling resonator [10, 11], defected ground [12], and meta-material structures [13, 14] are based on the partition principle. Neutralization approaches cancel the original coupling waves between antennas by rebuilding the additional wave paths with equal amplitude and opposite phase, such as decoupling grounds [15, 16], array antenna decoupling surface (ADS) [17], dielectric superstrate [18] and planar path [19]. The second type is the circuit domain decoupling method. Decoupling networks [20–22] construct the coupling signals through the feeding network in the circuit domain, which cancel out with the original coupling signals between the antennas. These methods can effectively improve the isolation; however, they are usually used for conventional antenna arrays rather than full-duplex antenna arrays. When considering full-duplex operation, the isolation between the transmitting and receiving antennas is important. In the full-duplex antenna array proposed in [23], only 30 dB isolation can be obtained. After increasing the antenna spacing, higher isolation ( $> 42$  dB) is obtained in [24]. In [25, 26], the interference between the transmitter and receiver is suppressed by integrating with the feeding network based on antiphase feeding technique. However, the transmitting and receiving antennas have orthogonal polarizations in above arrays [23–26], which is not applicable for some scenarios.

In this paper, a field-circuit combined decoupling method is proposed for co-polarized in-band full-duplex MIMO arrays. The proposed decoupling method consisting of the decoupling network and the ADS could construct the neutralization wave paths from circuit and field perspectives, respectively. An in-band full-duplex antenna with high isolation and low cross-polarization

Table 1: Performance comparison of full-duplex antenna arrays

Ref.	Pol.	Ant. Dis. ( $\lambda$ )	Isolation (TX/RX-RX/TX)	Coupling (TX/RX-TX/RX)
[23]	cross-pol.	0.57	> 30 dB	< -20 dB
[24]	cross-pol.	0.67	> 42 dB	< -25 dB
[25]	cross-pol.	0.50	> 50 dB	-
This work	co-pol.	0.56	> 47 dB	< -25 dB

level is designed and formed into a  $1 \times 4$  linear array with the spacing of  $0.56\lambda$  (where  $\lambda$  is the free-space wavelength at the working frequency). The decoupling network could alleviate the couplings between different antennas and the ADS could enhance the isolation in a single antenna. The  $1 \times 4$  full-duplex antenna array with the field-circuit combined decoupling method is fabricated and measured. At the working frequency of 2.6 GHz, both low coupling (< -25 dB) among the transmitting/receiving antennas and high isolation (> 47 dB) between the transmitting and receiving antennas are achieved. The performances of in-band full-duplex antenna arrays are compared in Table 1.

## II. FULL-DUPLEX ANTENNA ELEMENT

The configuration of the in-band full-duplex antenna is shown in Fig. 1, which is composed of a rectangular patch, four open-ended stubs, a fence-strip resonator (FSR), a metallic ground, and two dielectric layers. The dielectric substrates are made of F4B with a dielectric constant of 2.2 and a loss tangent of 0.001. The metallic strip is printed on the bottom side of the dielectric 1, and the patch and open-ended stubs are printed on the top side. The patch and strip are connected by series of metallic vias. The FSR structure consisting of metallic vias and strip is utilized to enhance the isolation between the TX and RX ports [4]. Two pairs of open-ended stubs are loaded to reduce the H-plane cross-polarizations of the shorted patch antennas [27]. Besides, the dimension of the antenna is reduced by using the rectangular slots on the patch. The TX and RX ports are excited by the symmetrical metallic probes, exhibiting the same linearly polarizations. The parameters of the antenna are listed in the caption of Fig. 1.

Figure 2 shows the simulated S-parameters of the full-duplex antenna. The reflection coefficients ( $S_{11}$  and  $S_{22}$ ) are lower than -10 dB, and the port isolation is above 30 dB at around 2.6 GHz. The simulated E-plane and H-plane radiation patterns for the TX and RX ports of the full-duplex antenna are shown in Fig. 3. As observed, the H-plane cross-polarization levels for both

ports maintain below -19.8 dB, and the satisfactory broadside radiated patterns are achieved.

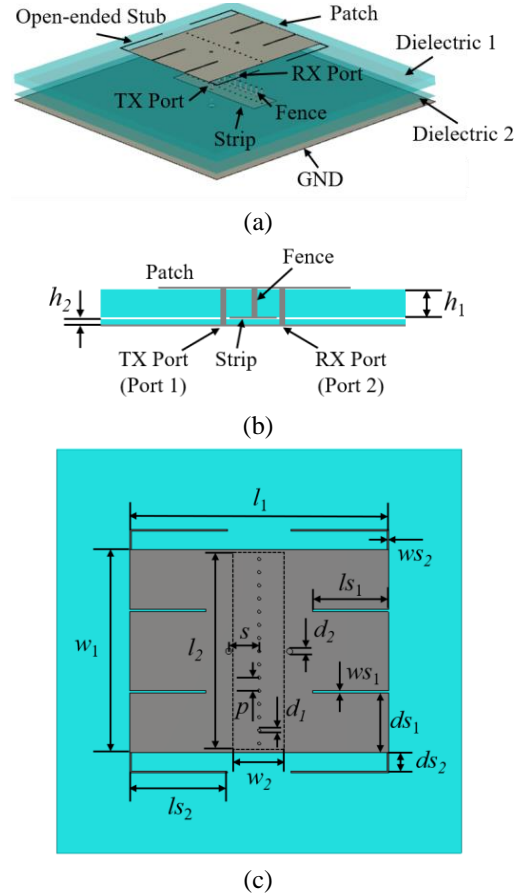


Fig. 1. Configuration of the full-duplex antenna. (a) Perspective view. (b) Side view. (c) Top view. The optimized parameters are:  $h_1 = 3$ ,  $h_2 = 0.165$ ,  $l_1 = 50$ ,  $l_2 = 40$ ,  $w_1 = 39$ ,  $w_2 = 10.4$ ,  $l_{s1} = 12.6$ ,  $l_{s2} = 19.2$ ,  $ws_1 = 0.5$ ,  $ws_2 = 0.3$ ,  $ds_1 = 11.25$ ,  $ds_2 = 4$ ,  $d_1 = 0.6$ ,  $d_2 = 1$ ,  $s = 6$ ,  $p = 2.6$  (all dimensions in mm).

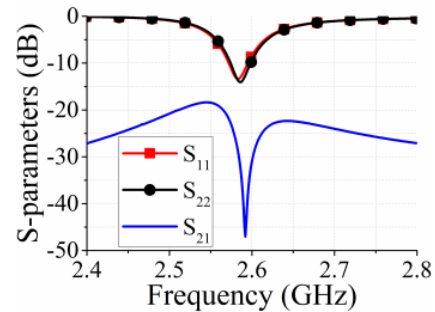


Fig. 2. Simulated S-parameters of the full-duplex antenna.

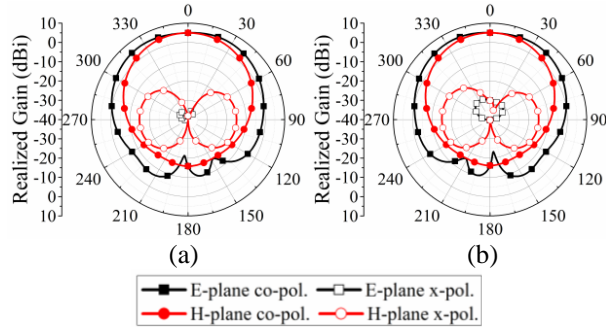


Fig. 3. Simulated radiation patterns of the full-duplex antenna at 2.58 GHz. (a) TX port. (b) RX port.

### III. FULL-DUPLEX ANTENNA ARRAY WITH FIELD-CIRCUIT COMBINED METHOD

#### A. Field-circuit combined method

The co-polarized in-band full-duplex antenna is expanded to a  $1 \times 4$  linear array with the element separation of 65 mm ( $0.56\lambda$ ), as shown in Fig. 4 (a). In such an array, both the coupling among transmitting/receiving antennas (e.g.,  $S_{13}$ ,  $S_{53}$ , and  $S_{73}$ ) and the isolation between transmitting and receiving antennas (e.g.,  $1/S_{23}$ ,  $1/S_{43}$ ,  $1/S_{63}$ , and  $1/S_{83}$ ) need to be considered. Figure 4 (b) shows the perspective view of the  $1 \times 4$  full-duplex antenna array with decoupling network, and the bottom view is shown in Fig. 4 (c). The microstrip transmission lines are printed on the bottom side of the dielectric substrate (made of 0.508 mm-thick Rogers RO4350B substrate with  $\epsilon_r = 3.66$  and  $\tan\delta = 0.0037$ ) below the ground layer. The apertures are etched on the metallic ground and placed below the patches' edges. Figure 4 (d) presents the array with decoupling network and ADS. The ADS is composed of a 1 mm-thick FR4 dielectric substrate (with  $\epsilon_r = 4.4$  and  $\tan\delta = 0.02$ ) and four rectangular metal radiator patches, which is arranged above the antenna array with a height of 3 mm. The final dimensions of the array and the decoupling structures are listed in the caption of Fig. 4.

The microstrip decoupling network at the feeding layer is provided for the linear array, as shown in Figs. 4 (b) and (c). The additional coupling wave from the feeding line of antenna element to adjacent antenna is generated by loading the apertures on the feeding lines [22]. The aperture coupling between the transmitting/receiving port and the adjacent transmitting or receiving port in different antenna is introduced from the circuit perspective, which is controlled by the size of the aperture. Since the apertures and feeding points of the radiating patches are connected by the feeding lines, the length and width of the microstrip transmission lines also need to be considered when decoupling. Therefore,

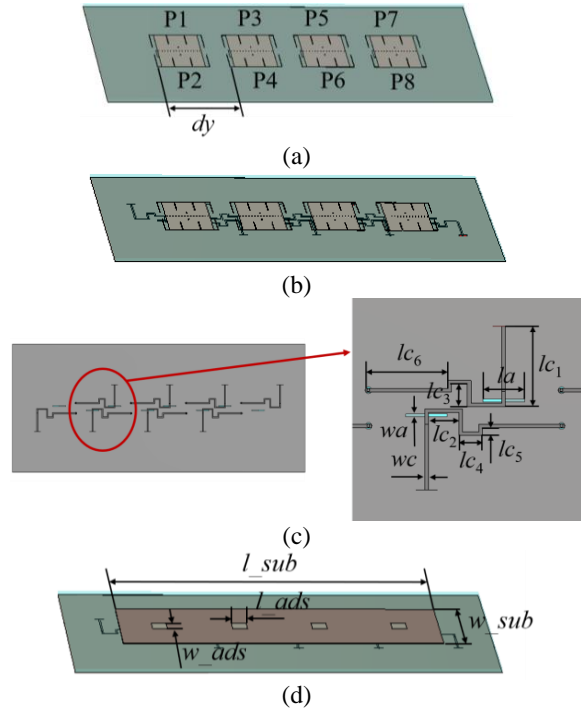


Fig. 4. Configuration of the  $1 \times 4$  full-duplex antenna array with/without the decoupling structures (decoupling network and ADS). (a) Perspective view of the array without decoupling structures (Array 1). (b) Perspective view of the array with decoupling network (Array 2). (c) Perspective view of the array with decoupling network and ADS (Array 3). (d) Bottom view of Array 3. The optimized dimensions are:  $dy = 65$ ,  $l_{sub} = 260$ ,  $w_{sub} = 65$ ,  $l_{ads} = 12$ ,  $w_{ads} = 12$ ,  $la = 14$ ,  $wa = 1$ ,  $lc_1 = 27.1$ ,  $lc_2 = 12.8$ ,  $lc_3 = 7.7$ ,  $lc_4 = 7.8$ ,  $lc_5 = 2.7$ ,  $lc_6 = 28.9$ ,  $wc = 1.2$  (all dimensions in mm).

the original couplings among different antenna elements can be neutralized by utilizing the aperture-loaded decoupling network.

Figure 5 shows the simulated S-parameters of the  $1 \times 4$  full-duplex antenna array with and without the decoupling network. Due to the page limit, only the S-parameters of the middle element of the array are shown here. As observed, after applying the decoupling network, the mutual couplings among neighboring transmitting/receiving antennas are effectively reduced from  $-19$  to  $-25$  dB or lower (see  $S_{13}$ ,  $S_{53}$ , and  $S_{73}$  in Fig. 5 (a)), while the isolations of the transmitting and receiving ports in different antennas ( $1/S_{23}$ ,  $1/S_{63}$ , and  $1/S_{83}$ ) are improved by around 12 dB (from 35 to 47 dB) at the working frequency of 2.6 GHz. The reflection coefficient of the antenna ( $S_{33}$ ) maintains below  $-10$  dB, and the isolation between the transmitting and receiving ports in a single antenna ( $1/S_{43}$ ) maintains above 30 dB.

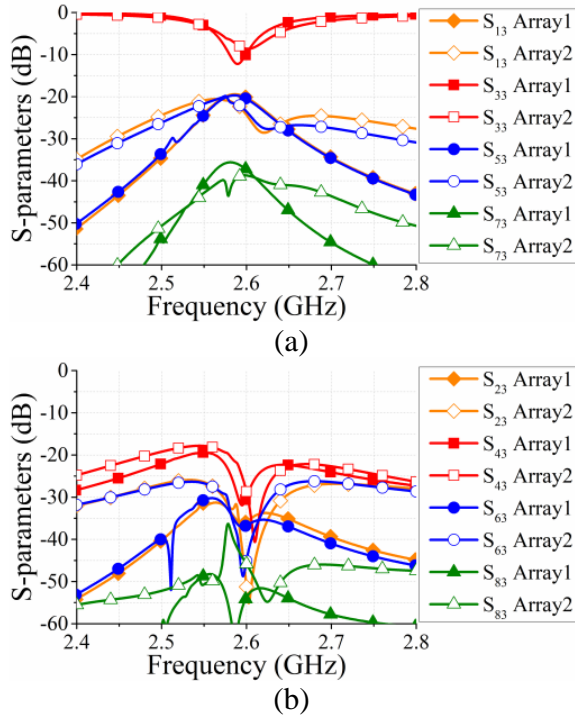


Fig. 5. Simulated S-parameters of the  $1 \times 4$  full-duplex antenna array with/without the decoupling network. (a)  $S_{13}$ ,  $S_{33}$ ,  $S_{53}$ , and  $S_{73}$ . (b)  $S_{23}$ ,  $S_{43}$ ,  $S_{63}$ , and  $S_{83}$ .

Thus, the decoupling networks can significantly suppress the couplings among different antennas, but have little effect on the port isolation in a single antenna. To improve the isolation between the transmitting and receiving ports in a single antenna, the ADS structure is employed for the array with the decoupling network, as electromagnetic waves radiated by the transmitting antenna are reflected by the metal reflector and received by the receiving antenna in the same element, forming an additional coupling wave path from the field perspective [17]. The amplitude and phase of the additional wave path are determined by the height and the size of the metal reflectors. Thus, the original coupling between transmitting and receiving ports in a single antenna can be counteracted by employing the ADS.

Figure 6 shows the simulated S-parameters of the  $1 \times 4$  full-duplex antenna array with and without the decoupling network and ADS. It is obvious that, with the decoupling network and ADS, the isolation between the transmitting and receiving ports in a single antenna is significantly improved from 30 to 50 dB at the working frequency of 2.6 GHz (see  $1/S_{43}$  in Fig. 6 (a)). The couplings among neighboring transmitting/receiving antennas ( $S_{13}$ ,  $S_{53}$ , and  $S_{73}$ ) remain below  $-25$  dB, while the isolations of the transmitting and receiving ports in different antennas ( $1/S_{23}$ ,  $1/S_{63}$ , and  $1/S_{83}$ ) remain larger

than 47 dB. Meanwhile, the reflection coefficient of the antenna ( $S_{33}$ ) continues below  $-10$  dB. Therefore, after loading the ADS structure, the isolation between the transmitting and receiving ports in a single antenna is effectively enhanced while maintaining the other high isolations between different antennas. Figure 7 presents the simulated normalized E-plane and H-plane radiation patterns of TX port (P3) with and without the decoupling network and ADS. As can be seen, the radiation patterns

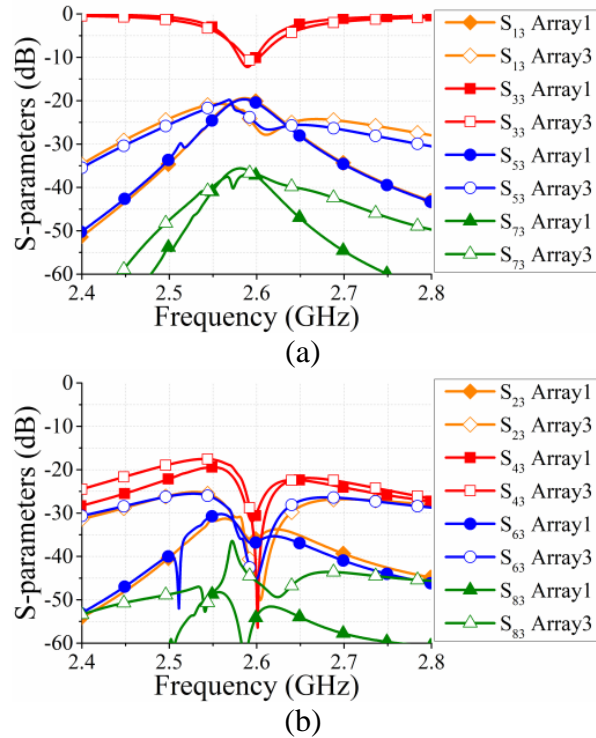


Fig. 6. Simulated S-parameters of the  $1 \times 4$  full-duplex antenna array with/without the decoupling network and ADS. (a)  $S_{13}$ ,  $S_{33}$ ,  $S_{53}$ , and  $S_{73}$ . (b)  $S_{23}$ ,  $S_{43}$ ,  $S_{63}$ , and  $S_{83}$ .

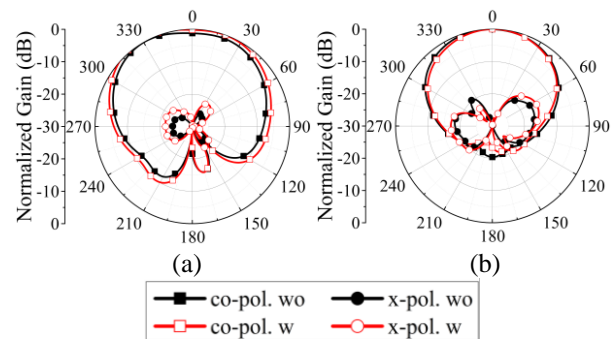


Fig. 7. Simulated normalized radiation patterns of TX port (P3) with/without the decoupling network and ADS. (a) E-plane. (b) H-plane.

with the decoupling network and ADS are comparable to the original patterns, exhibiting low cross-polarization level ( $< -14.5$  dB) and satisfactory radiation performances.

It is concluded that all the isolations of the co-polarized in-band full-duplex antenna array can be significantly enhanced by employing the decoupling network and ADS. The proposed field-circuit combined decoupling method combines the circuit domain decoupling network and the field domain ADS structure to simultaneously obtain lower coupling between the transmitting/receiving antennas and higher isolation between transmitting and receiving antennas.

**B. Measurement results**

Figure 8 shows the prototype photos of the  $1 \times 4$  full-duplex antenna array with the field-circuit combined method. The decoupling network and the ADS structure are employed in the array. The ADS and the substrate layers are fixed together using Nylon screws.

The simulated and measured S-parameters of the  $1 \times 4$  full-duplex antenna array using the field-circuit combined method are presented in Fig. 9. It is clear that, at the working frequency of 2.6 GHz, the coupling between the transmitting/receiving antennas is about  $-25$  dB or lower, while the coupling between the transmitting and receiving antennas is lower than  $-47$  dB. The measurement results are comparable to the simulation results. The small discrepancies are caused by imperfect soldering, manufacturing tolerance, and measurement errors. Figure 10 shows the simulated and measured E-plane and H-plane radiation patterns of TX port (P3) using the field-circuit combined method. Low cross-polarization level ( $< -14.5$  dB) and satisfactory radiation perfor-

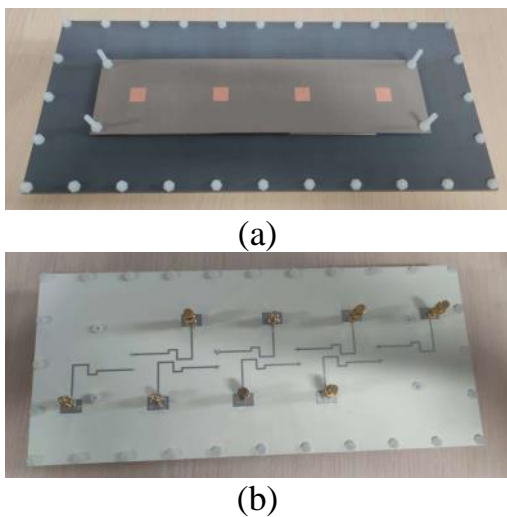


Fig. 8. Photographs of the prototype. (a) Top view. (b) Bottom view.

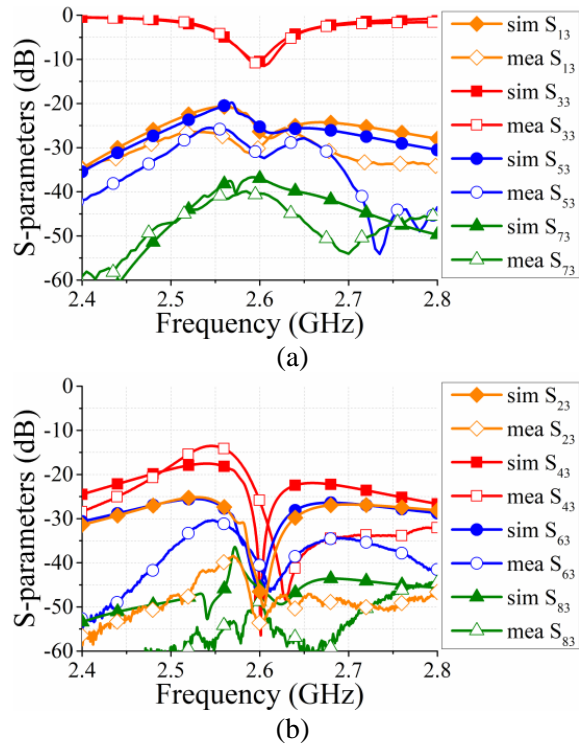


Fig. 9. Simulated and measured S-parameters of the  $1 \times 4$  full-duplex antenna array using the field-circuit combined method (decoupling network and ADS). (a)  $S_{13}$ ,  $S_{33}$ ,  $S_{53}$ , and  $S_{73}$ . (b)  $S_{23}$ ,  $S_{43}$ ,  $S_{63}$ , and  $S_{83}$ .

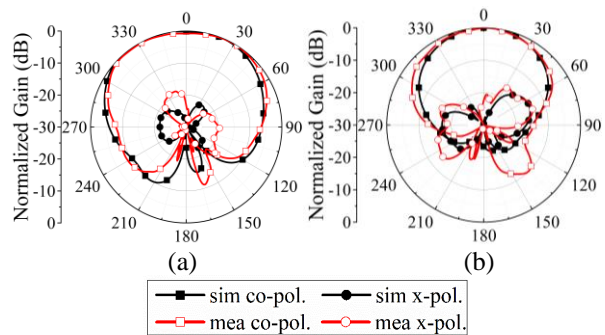


Fig. 10. Simulated and measured radiation patterns of TX port (P3) using the field-circuit combined method (decoupling network and ADS). (a) E-plane. (b) H-plane.

mances are obtained. Meanwhile, the simulated and measured radiation patterns are in good agreement.

**IV. CONCLUSION**

A field-circuit combined decoupling method consisting of the decoupling network and ADS was presented in this paper. The additional coupling waves in the circuit and field domains were generated to cancel the original couplings. An in-band full-duplex

antenna with the same polarization was designed and formed into a  $1 \times 4$  linear array. The coupling between different antennas could be suppressed by the decoupling network, and the isolation in a single antenna could be enhanced by the ADS. The  $1 \times 4$  array, together with the decoupling network and the ADS, have been manufactured and experimented. The simulated and measured results were in reasonable consistent. Low coupling ( $< -25$  dB) among the transmitting/receiving antennas and high isolation ( $> 47$  dB) between the transmitting and receiving antennas were achieved at 2.6 GHz. Therefore, the proposed field-circuit combined decoupling method could be used for enhancing the isolations of co-polarized in-band full-duplex MIMO arrays.

### ACKNOWLEDGMENT

This work was supported by the National Key Research and Development Program of China under Grant 2022YFB3902400.

### REFERENCES

- [1] A. Sabharwal, P. Schniter, D. Guo, D. W. Bliss, S. Rangarajan, and R. Wichman, "In-band full-duplex wireless: Challenges and opportunities," *IEEE J. Sel. Areas Commun.*, vol. 32, no. 9, pp. 1637-1652, Sep. 2014.
- [2] D. Kim, H. Lee, and D. Hong, "A survey of in-band full-duplex transmission: From the perspective of PHY and MAC layers," *IEEE Commun. Surv. Tuts.*, vol. 17, no. 4, pp. 2017-2046, 2015.
- [3] W. Zhang, J. Hu, Y. Li, and Z. Zhang, "Design of a stacked co-polarized full-duplex antenna with broadside radiation," *IEEE Trans. Antennas Propag.*, vol. 69, no. 11, pp. 7111-7118, Nov. 2021.
- [4] Y. He and Y. Li, "Compact co-linearly polarized microstrip antenna with fence-strip resonator loading for in-band full-duplex Systems," *IEEE Trans. Antenn. Propag.*, vol. 69, no. 11, pp. 7125-7133, Nov. 2021.
- [5] J. H. Zhang, F. M. He, W. Li, and Y. Li, "Self-interference cancellation: A comprehensive review from circuits and fields perspectives," *Electron.*, vol. 11, no. 2, pp. 172, Jan. 2022.
- [6] F. Peng, F. Yang, B. Liu, and X. Chen, "Experimental investigation of decoupling effect on the nonlinearity of power amplifiers in transmitter array," *Applied Computational Electromagnetics Society (ACES) Journal*, in press.
- [7] X. Chen, S. Zhang, and Q. Li, "A review of mutual coupling in MIMO systems," *IEEE Access*, vol. 6, pp. 24706-24719, Apr. 2018.
- [8] Z. Zhang, K. Long, A. V. Vasilakos, and L. Hanzo, "Full-duplex wireless communications: challenges, solutions, and future research directions," *Proc. IEEE*, vol. 104, no. 7, pp. 1369-1409, Jul. 2016.
- [9] S. B. Venkatakrishnan, A. Hovsepian, A. D. Johnson, T. Nakatani, E. A. Alwan, and J. L. Volakis, "Techniques for achieving high isolation in RF domain for simultaneous transmit and receive," *IEEE Open J. Antennas Propag.*, vol. 1, pp. 358-367, Jul. 2020.
- [10] M. Li, X. Chen, A. Zhang, W. Fan, and A. A. Kishk, "Split-ring resonator-loaded baffles for decoupling of dual-polarized base station array," *IEEE Antennas Wirel. Propag. Lett.*, vol. 19, no. 10, pp. 1828-1832, Oct. 2020.
- [11] F. Faraz, X. Chen, Q. Li, J. Tang, J. Li, T. A. Khan, and X. Zhang, "Mutual coupling reduction of dual polarized low profile MIMO antenna using decoupling resonators," *Applied Computational Electromagnetics Society (ACES) Journal*, vol. 35, no. 1, pp. 38-43, Jan. 2020.
- [12] B. Qian, X. Chen, and A. A. Kishk, "Decoupling of microstrip antennas with defected ground structure using the common/differential mode theory," *IEEE Antennas Wirel. Propag. Lett.*, vol. 20, no. 5, pp. 828-832, May 2021.
- [13] K. Yu, Y. Li, and X. Liu, "Mutual coupling reduction of a MIMO antenna array using 3-D novel meta-material structures," *Applied Computational Electromagnetics Society (ACES) Journal*, vol. 33, no. 7, pp. 758-763, Jul. 2018.
- [14] S. Luo, Y. Li, Y. Xia, and L. Zhang, "A low mutual coupling antenna array with gain enhancement using metamaterial loading and neutralization line structure," *Applied Computational Electromagnetics Society (ACES) Journal*, vol. 34, no. 3, pp. 411-418, Mar. 2019.
- [15] S. Zhang, X. Chen, and G. F. Pedersen, "Mutual coupling suppression with decoupling ground for massive MIMO antenna arrays," *IEEE Trans. Veh. Technol.*, vol. 68, no. 8, pp. 7273-7282, Aug. 2019.
- [16] S. Song, X. Chen, Y. Da, and A. A. Kishk, "Broadband dielectric resonator antenna array with enhancement of isolation and front-to-back ratio for MIMO application," *IEEE Antennas Wirel. Propag. Lett.*, vol. 21, no. 7, pp. 1487-1491, Jul. 2022.
- [17] K. Wu, C. Wei, X. Mei, and Z. Y. Zhang, "Array-antenna decoupling surface," *IEEE Trans. Antennas Propag.*, vol. 65, no. 12, pp. 6728-6738, Dec. 2017.

- [18] Y. Da, Z. Zhang, X. Chen, and A. A. Kishk, "Mutual coupling reduction with dielectric superstrate for base station arrays," *IEEE Antennas Wirel. Propag. Lett.*, vol. 20, no. 5, pp. 843-847, May 2021.
- [19] L. Gu, W. Yang, S. Liao, Q. Xue, and W. Che, "Novel coupling cancellation method by loading planar path for wideband high-isolation wide-scanning millimeter-wave phased array," *IEEE Trans. Antennas Propag.*, vol. 70, no. 11, pp. 10520-10530, Nov. 2022.
- [20] T. Dong and K. K. M. Cheng, "Compact antenna array with newly designed decoupling network," *Applied Computational Electromagnetics Society (ACES) Journal*, vol. 33, no. 11, pp. 1196-1200, Nov. 2018.
- [21] X. J. Zou, G. M. Wang, Y. W. Wang, and H.-P. Li, "An efficient decoupling network between feeding points for multielement linear arrays," *IEEE Trans. Antennas Propag.*, vol. 67, no. 5, pp. 3101-3108, May 2019.
- [22] Y. M. Zhang and S. Zhang, "A novel aperture-loaded decoupling concept for patch antenna arrays," *IEEE Trans. Microw. Theory Techn.*, vol. 69, no. 9, pp. 4272-4283, Sep. 2021.
- [23] M. V. Kuznetsov, S. K. Podilchak, A. J. McDermott, and M. Sellathurai, "Dual-polarized high-isolation antenna design and beam steering array enabling full-duplex communications for operation over a wide frequency range," *IEEE Open J. Antennas Propag.*, vol. 2, pp. 521-532, Mar. 2021.
- [24] M. V. Kuznetsov, S. K. Podilchak, A. J. McDermott, and M. Sellathurai, "Dual-polarized antenna with dual-differential integrated feeding for wideband full-duplex systems," *IEEE Trans. Antennas Propag.*, vol. 69, no. 11, pp. 7192-7201, Nov. 2021.
- [25] Y. M. Zhang, S. Zhang, J. L. Li, and G. F. Pedersen, "A dual-polarized linear antenna array with improved isolation using a slotline-based 180° hybrid for full-duplex applications," *IEEE Antennas Wirel. Propag. Lett.*, vol. 18, no. 2, pp. 348-352, Feb. 2019.
- [26] D. Wójcik, M. Surma, A. Noga, and M. Magnuski, "High port-to-port isolation dual-polarized antenna array dedicated for full-duplex base stations," *IEEE Antennas Wirel. Propag. Lett.*, vol. 19, no. 7, pp. 1098-1102, Jul. 2020.
- [27] N. W. Liu, L. Zhu, Z. X. Liu, Z. Y. Zhang, G. Fu, and Y. Liu, "Cross-polarization reduction of a shorted patch antenna with broadside radiation

using a pair of open-ended stubs," *IEEE Trans. Antennas Propag.*, vol. 68, no. 1, pp. 13-20, Jan. 2020.



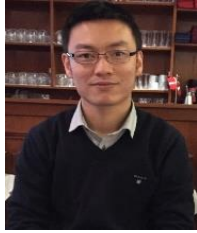
**Yiran Da** received the B.S. degree in Information Engineering from Xi'an Jiaotong University, Xi'an, China, in 2020, where she is currently pursuing the M.S. degree. Her research interests include base station antenna design and mutual coupling reduction.



**Jianjia Yi** (Member, IEEE) received the B.S. degree in Electrical Engineering from the Harbin Institute of Technology, Harbin, China, in 2009, the M.S. degree in Telecommunication Engineering from Politecnico di Torino, Turin, Italy, in 2012, and the Ph.D. degree in Physics from University Paris Saclay, Paris, France, in 2015. From 2016 to 2019, he was an Associate Professor with the State Key Laboratory of Integrated Services Networks, School of Telecommunications Engineering, Xi'dian University, Xi'an, China. He is currently an Associate Professor with Xi'an Jiaotong University, Xi'an. He has coauthored two book chapters and more than 60 articles in peer-reviewed international journals and conference proceedings. His research interests include theoretical and computational electromagnetics with applications to antenna theory and design, antennas, frequency-selective surfaces, transmitarray, and metagratings.



**Jianxing Li** (S'15-M'18) received the B.S. degree in Information and Communications Engineering, and the M.S. and Ph.D. degrees in Electromagnetic Field and Microwave Techniques, all from Xi'an Jiaotong University, Xi'an, China, in 2008, 2011, and 2016, respectively. From 2014 to 2016, he was a visiting researcher with the Department of Electrical and Computer Engineering, Duke University, Durham, NC, USA. He is currently an associate professor at Xi'an Jiaotong University. His research interests include microwave and mmWave circuits and antennas, wireless power transfer, and multi-functional mmWave antennas.



**Xiaoming Chen** (M'16–SM'19) received the B.Sc. degree in electrical engineering from Northwestern Polytechnical University, Xi'an, China, in 2006, and M.Sc. and PhD degrees in electrical engineering from Chalmers University of Technology, Gothenburg, Sweden, in 2007 and 2012, respectively. From 2013 to 2014, he was a postdoctoral researcher at the same University. From 2014 to 2017, he was with Qamcom Research & Technology AB, Gothenburg, Sweden. Since 2017, he has been a professor at Xi'an Jiaotong University, Xi'an, China. His research areas include MIMO antennas, over-the-air testing, reverberation chambers, and hardware impairments and mitigation. Prof. Chen serves as a Senior Associate Editor (AE) for IEEE Antennas and Wireless Propagation Letters and received the Outstanding AE Awards in 2018, 2019, 2020, and 2021. He received the URSI (International Union of Radio Science) Young Scientist Awards in 2017 and 2018.